Two-photon absorption switches based on protonation of pyrimidine derivatives

Lampros Sdralias, Alexandros Katsidas, Ioannis Polyzos, Thibault Bonnaud, Guillaume Noirbent, Sylvain Achelle, Mihalis Fakis

Two-Photon Absorption Switches Based on Protonation of Pyrimidine Derivatives

Lampros Sdralias,[a] Alexandros Katsidas,[a] Ioannis Polyzos,[a] Thibault Bonnaud,[b] Guillaume Noirbent,[b] Sylvain Achelle,[b,*] Mihalis Fakis[a,*]

[a] Department of Physics, University of Patras, GR-26500, Greece
E-mail: fakis@upatras.gr

[b] Univ Rennes, CNRS ISCR (Institut des Sciences Chimiques de Rennes)
UMR 6226, F-35000, Rennes, France
E-mail : sylvain.achelle@univ-rennes.fr

Abstract: The photophysical and two-photon absorption (TPA) properties of five push-pull pyrimidine derivatives were studied upon protonation with trifluoroacetic acid (TFA). The pyrimidine heterocycles have been used as the protonation sites and electron acceptors while methoxy groups were employed as electron donors. Steady state and fluorescence time-resolved spectroscopy from femtoseconds to nanoseconds have been used together with the two-photon excited fluorescence method. Protonation with TFA resulted in red-shifted absorption and fluorescence spectra as well as to an acceleration of the excited state dynamics. The TPA properties showed a remarkable enhancement upon protonation with a ten-times increase of the TPA cross sections due to an increased intramolecular charge transfer. Our results demonstrate the potential of pyrimidine chromophores to be used as protonation tunable non-linear optical chromophores.

Introduction

Two-photon absorption (TPA) is a 3rd order nonlinear optical phenomenon that is related to the simultaneous absorption of two photons.[1,2] TPA is quantitatively linked to the imaginary part of γ, the cubic hyperpolarisability tensor and is only observed when suitable materials are illuminated by sufficiently powerful sources of coherent light (pulsed lasers of fs or ps pulse duration) showing a quadratic dependance on excitation intensity. In case of fluorescent TPA chromophores, the TPA excitation results in emission of photons of higher energy than excitation photons. Two-photon excitation fluorescence (TPEF) is a powerful method to measure the TPA cross sections of fluorescent media.[3,4] Although it is considered an indirect method to measure the TPA properties, its main advantage over direct methods based on non-linear transmission is the capability to monitor the order of the non-linearity (in order to avoid undesired effects and artifacts due to thermal phenomena, scattering, self-absorption, higher order non-linearities etc) and the use of low concentrations. [5] Organic materials exhibiting TPA are generally based on push-pull structures of dipolar, quadrupolar and octupolar topology, exhibiting significant intramolecular charge transfer (ICT).[1,2,6,7,8,9] The main applications of TPA are related to bioimaging,[10,11,12,13] photodynamic therapy,[14,15, 16] optical limiting.[17,18,19] microfabrication,[20,21,22,23] and 3D optical data storage.[24,25,26] The first two ones take advantage of the near infrared excitation reducing biological tissues absorption and scattering, while the last ones take advantage to the fact that TPA occurs only at the focal point of the laser within a volume of 100 femtoliters, generating highly localized photophysical or photochemical phenomena with a spectral resolution of 100 nm.

The studies of chromophores combining TPA and chromism are rather scarce in the literature. Few examples of photochromism induced by two-photon excitation have been described.[27,28,29] Belfield et al have designed 4-styrylguaiazulene exhibiting efficient fluorescence switch-on upon protonation.[30] These chromophores have been efficiently used in systems for two-photon microlithography with iodonium photoacid generator in polymethyl methacrylate. However, to the best of our knowledge, the protonation has never been used to tune the spectrum of TPA and increase the TPA cross section values.

Push-pull pyrimidine chromophores, including styrylpyrimidine groups, are known for their strong luminescence properties and have found applications as fluorescent sensors and emitters for organic light emitting diodes.[31,32,33,34,35] Styrylpyrimidines are also well-known for their TPA properties and have been efficiently used in various applications.[36,37,38,39,40,41,42] However, the amino substituted styrylpyrimidines have been almost exclusively studied for their TPA properties.[24] A significant branching effect was observed with significantly stronger TPA cross section for 4,6-distyryl- and 2,4,6-tristyrylpyrimidines than for their 4-monostyryl analogues (Scheme 1).[43,44] Pyrimidine push-pull chromophores have also been described for their sensibility to pH (halochromism).[45] The protonation of the pyrimidine ring significantly increases its electron-withdrawing character. In case of 4-styrylpyrimidines, it has been calculated that the protonation

occurs exclusively on the N1 atom. [46,47] The pyrimidine ring acts as a monobase with pKa ≈ 1.1. The protonation of the first nitrogen atom leads to a marked decrease in the basicity of the second nitrogen atom due to the attractive inductive effect of the resulting quaternary nitrogen (pKa ≈-6.3), as a consequence a double protonation by TFA is not envisioned. [45] Depending on the nature of electron-donating group, the protonation induced either an emission quenching or a red-shifted emission. In the case of methoxy substituted styrylpyrimidines, with extended π-conjugated linker, an emission color change from blue to orange/red can be achieved when acid is added while white light is observed upon partial protonation.[48] Both neutral and protonated forms exhibit significant fluorescence quantum yield. Besides, the absorption spectra of pyrimidine chromophores exhibit a clear bathochromic shift upon protonation which triggered us to examine the effect of protonation on the TPA spectra.

Therefore, we report here on the effect of protonation on photophysics as well as on the TPA properties of five methoxy substituted pyrimidines **1**-**5** (Scheme 2). A significant increase of the TPA cross sections was observed leading to protonation controlled TPA switches. This is due to enhanced ICT upon protonation, indicating stronger electron accepting ability of the protonated pyrimidine group.

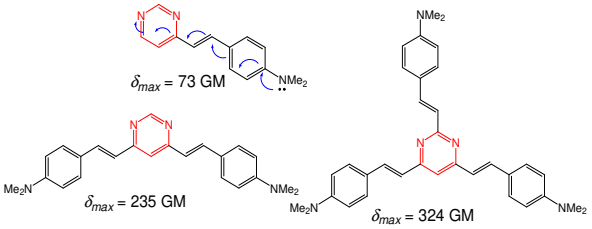

Scheme 1. Structure of few styrylpyrimidine chromophores and their TPA properties from ref 43. ICT is symbolized by blue arrows on the structure of monostyryl chromophore.

Results and Discussion

Materials

The herein studied five molecules are shown in scheme 2. They are of dipolar (**1**-**3**) or quadrupolar (**4**, **5**) nature. They bear pyrimidine electron withdrawing and methoxy electron donating groups. Their synthesis was described previously by some of us.[46,49,50,51] Compounds **1**-**4** are highly soluble in common organic solvents (DCM, $CHCl_3$, THF). The solubility of **5** is limited but solutions up to 10^{-3}M can be obtained.

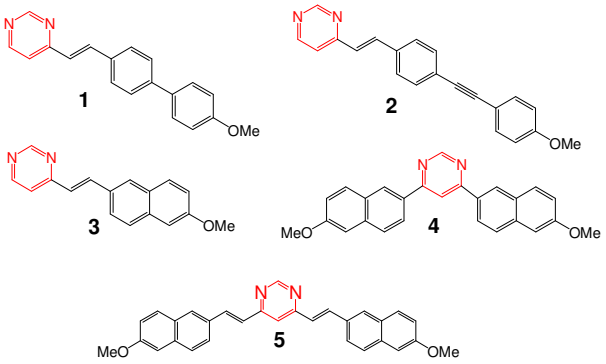

Scheme 2. Structure of chromophores **1**-**5**.

Steady state spectroscopy

The steady state spectra of the five chromophores have been studied in neutral form in dichloromethane (DCM) solutions as well as in protonated form in acidified DCM (10^{-2}M TFA). Table 1 summarizes the photophysical results. In several previous works, the systematic change of the photophysical properties of azaheterocxyclic protonable chromophores has been studied in details focusing on the emission of dual fluorescence and white light generation via a partial energy transfer and by combining emission by both neutral and protonated species.[48-50,52,53,54,55] That was achieved by means of a careful addition of tiny amounts of acid. However, here we only study the different properties of the neutral and the fully protonated molecules in acidified solvents, focusing on the excited state dynamics and TPA properties. In neutral form, the five chromophores show a low-energy absorption peak in the range of 338-380 nm with molar absorption coefficients ranging

Table 1. Photophysical parameters of compounds **1**-**5** in DCM and acidified DCM (10^{-2}M TFA).

Compound	DCM		TFA 10^{-2}M in DCM	
	λ_{abs}/nm (ε/mM^{-1} cm^{-1})	λ_{em}/nm (Φ_F)	λ_{abs}/nm (ε/mM^{-1} cm^{-1})	λ_{em}/nm (Φ_F)
1	346 (33.2)	447 (0.14)	417 (19.7)	578 (0.15)
2	285 (11.4), 351 (28.8)	458 (0.51)	286 (13.1), 404 (23.5)	597 (0.15)
3	276 (13.1), 345 (20.6)	443 (0.022)	281sh (9.9), 425 (15.4)	558 (0.30)
4	268 (55.9), 338 (38.1)	415 (0.90)	263 (43.2), 427 (37.1)	531 (0.70)

from 20 mM^{-1}cm^{-1} up to 39 mM^{-1}cm^{-1} (Figure 1a). In the protonated form, these peaks disappear while new red-shifted peaks in the range 404-482 nm emerge, attributed to charge transfer from methoxy to the pyrimidine group (Figure 1a) which after the protonation has an increased electron-withdrawing character.[48] The fluorescence spectra show initial peaks of the neutral species at 415-470 nm (Figure 1b). The spectra are structureless and broad without any vibronic peaks. This is due to the flexible nature of the solutes and the polarity of the solvent (dielectric constant of 8.93). In acidified DCM, the fluorescence of the neutral molecules almost vanishes, while only weak shoulders appear in some cases due to emission from the remaining neutral molecules (Figure 1b). New peaks are formed in the range 531-597 nm which point to a red-shifted emission from the protonated chromophores.[48] Again, these spectra are structureless and even broader than those of neutral molecules as expected for emission by CT states.[56,57] The quantum yields (Φ_F) are moderate to very high for the neutral molecules **1**, **2**, **4** and **5** while it is extremely low for **3**. On the other hand, the protonated forms of all compounds exhibit Φ_F higher than 0.15 up to 0.70.

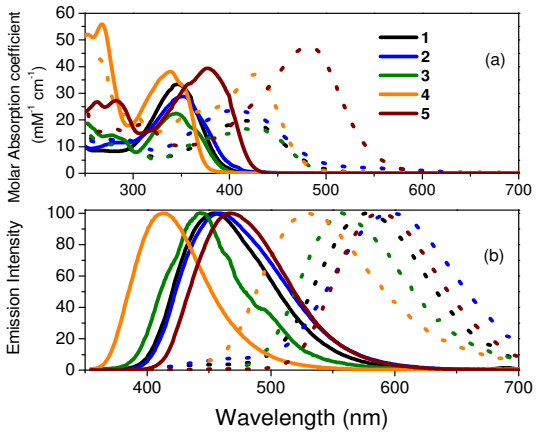

Figure 1. Absorption spectra (a) and normalized emission spectra (b) of compounds **1**-**5** (5 ×10^{-6}M) in DCM (solid lines) and acidified DCM (10^{-2}M TFA) (dashed lines). The emission spectra were detected upon excitation at the absorption maxima.

Time-resolved spectroscopy

The fluorescence dynamics have been studied by the femtosecond (fs) upconversion and time-correlated single photon counting (TCSPC) methods focusing on the temporal range of a few picoseconds (ps) and hundreds of nanoseconds (ns) respectively. Measurements were taken in both the fluorescence bands of the neutral and protonated species in an effort to understand the induced changes in the excited states upon protonation. In the fs upconversion method, the excitation beam was tuned either to 380 or 420 nm to excite the neutral and protonated species respectively while in the TCSPC technique, the excitation wavelength was 400 nm. Figures 2 and 3 show the early dynamics within the first 40 ps for **2** and **5**. Compound **2** does not exhibit any fast decay dynamics in the first few ps when detected at the peak of the neutral emission band (460 nm) in DCM (figure 2a). A slow rise within the first 2 ps is due to a structural relaxation and solvation, accompanied by ICT mechanism (see figure S1 for a complete set of dynamics at different emission wavelengths showing a dip and rise behavior on the few ps timescale, leading to a transient red-shift of the emission spectrum).[42,58,59,60.] However,

in acidified DCM and at the same high-energy emission band, it shows an ultrafast decay of <100 fs pointing to the dynamic quenching of the remaining neutral species. The dynamics at the protonated red-shifted band (600 nm) were detected for two cases i.e for a slightly and a fully protonated acidified solution (figure 2b). The slightly protonated molecules were prepared by adding 10 eq. of TFA in the original DCM solution. According to ref. 48, 10 eq. of TFA is a small quantity that only slightly protonates the molecules, while on the other hand in the acidified DCM, all molecules are considered to exist in their protonated form. Within the first 40 ps, the fully protonated species decay faster than the slightly protonated ones (with a lifetime of the order of 10 ps). This is ascribed to the enhanced CT experienced in the former species leading to enhanced non-radiative transitions.

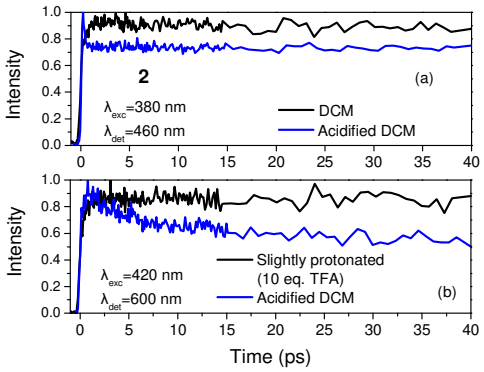

Figure 2. Early fluorescence dynamics of **2** detected at the emission band of the neutral (a) and protonated species (b).

Similar results were obtained for **5** as shown in Figure 3. However, addition of TFA only leads to a slightly faster initial decay of the neutral species at 470 nm (figure 3a), i.e. the effect of TFA on the excited state dynamics is less significant than in the case of **2**, indicating the presence of a static quenching mechanism of the neutral molecules of **5** by TFA. In the protonated band (590 nm), the decay of the fully protonated molecules again becomes faster pointing to enhanced non-radiative transitions, exhibiting similar dynamics to **2** on the tens of ps timescale.

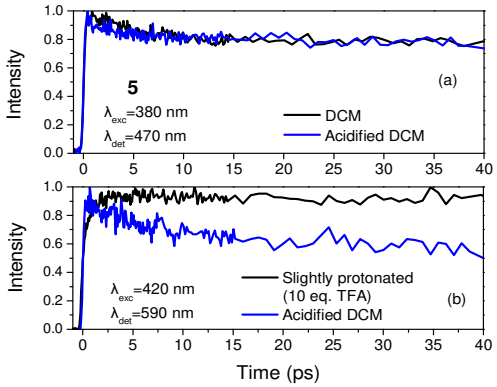

Figure 3. Early fluorescence dynamics of **5** detected at the emission band of the neutral (a) and protonated species (b).

The corresponding early dynamics for the other three molecules are presented in Figures S2-S4. Compound **1** follows an ultrafast (<100 fs) decay in acidified DCM when detected at the high energy neutral emission band showing similar behavior to **2**. For **3** and **4**, the dynamics were detected only at the protonated band (530 and 560 nm) upon 420 nm excitation because the signal at the neutral emission band was too low to be detected. Both compounds showed acceleration of the decays upon increasing the strength of protonation.

Although the early dynamics provide significant information on the deactivation process upon adding TFA, a detailed quantitative analysis of the change of the lifetimes was made upon detecting on the ns timescale (Figures 4, 5 and S5-S7). Figure 4a shows the decay of **2** at 460 nm before and after adding TFA. In its neutral form (detection at 460 nm), **2** decays monoexponentially with a single lifetime of 1.14 ns (Table S1 presents the fitting results of the ns fluorescence

dynamics for all compounds). Addition of TFA leads to a very fast initial decay of < 0.05 ns (within the response functions of our system), dominating the dynamics, and a slower one (1.13 ns) attributed to the remaining neutral species. The dynamics of the protonated species, detected at 600 nm, are bi-exponential with lifetimes of 1.50 and 1.98 ns for the slightly protonated sample (Figure 4b). However, in the fully protonated case, the dynamics are accelerated and become mono-exponential with a lifetime of 0.68 ns. This acceleration was also obvious in the fs measurements, as discussed above and is due to the stronger electron accepting ability of the protonated pyrimidine group.[61,62,63] It is also related to a decrease in the fluorescence intensity of the protonated species while it can also be associated to the increase of the polarity of the solution (Figure S8).

The neutral species of **5** show a different excited state dynamics upon titrating with acid (Figure 5). Initially, a bi-exponential decay was observed for the neutral species with lifetimes of 0.37 and 1.38 ns (470 nm). After adding TFA, the decay lifetimes only slightly change while the amplitude of the fast/slow component increases/decreases leading to an overall decrease of the average lifetime from 1.21 to 0.90 ns. Therefore, an abrupt decrease of the lifetime as in **2** is absent. This slight change in the dynamics was also observed in the fs measurements (Figure 3). The protonated species of **5** follow the discussion given above for **2** showing a decrease of the lifetime (figure 5b).

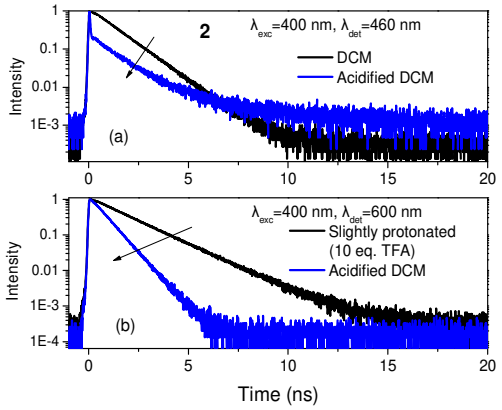

Figure 4. Nanosecond fluorescence dynamics of **2** detected at the emission band of the neutral (a) and protonated species (b).

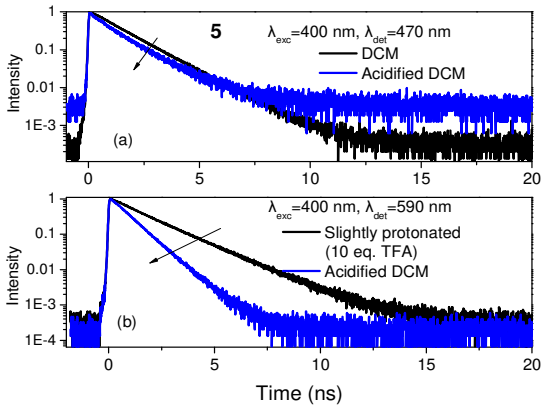

Figure 5. Nanosecond fluorescence dynamics of **5** detected at the emission band of the neutral (a) and protonated species (b).

The nanosecond dynamics for compounds **1**, **3** and **4** are shown in figures S5-S7. Among all five molecules, **3** has a totally discrete dynamic. In neutral form, **3** decays rapidly with a main lifetime of 0.06 ns (Table S1) which is related to its very small Φ_F (Table 1). This lifetime becomes even smaller upon adding TFA while the longer mechanism that is observed is due to the emission by the protonated species (Figure S7a). Compound **1** also exhibits a small neutral lifetime of 0.34 ns which is also related to its reduced Φ_F (Tables S1 and 1) and again becomes significantly faster upon adding TFA.

Two-photon absorption

The TPA properties of compounds **1**-**5** have been studied in neutral form in DCM solutions and the results are shown in Figure 6. In all cases, the quadratic law for a two-photon excitation has been validated and corresponding results are given in Figure S9. Low δ_{TPA} values have been achieved with values below 100 GM while only **5**, having a quadrupolar and elongated structure, showed moderate values reaching 150 GM having in mind that all compounds are expected to exhibit their TPA maxima close to 700-720 nm which is not within our experimental range. In their protonated form, all molecules showed remarkably enhanced TPA properties and red-shifted spectra (figure 6). Table S2 summarizes all TPA data for the neutral and protonated species. The two quadrupolar molecules **4** and **5** showed the largest TPA action cross sections ($\Phi_F \times \delta_{TPA}$) reaching 200 and 350 GM respectively (figure 6a). The TPA spectrum of **5** is red-shifted compared to that of **4** as expected by its elongated structure and one-photon absorption (OPA) spectrum. Compound **5** also exhibited maximum δ_{TPA} of about 2000 GM after dividing with Φ_F i.e. excellent values compared to similar compounds.[64,65,66,67,68,69,70] A comparison of the TPA spectra with the rescaled OPA is given in figure S11 for **1** and **5**. Compound **1** shows matched TPA and OPA spectra as expected by its dipolar D-π-A structure. On the other hand, for quadrupolar molecules like **5** where the excited state splits to form two new states, the TPA spectrum is expected to be blue shifted compared to the rescaled OPA one, pointing to higher energy TPA excitations.[71] The spectra in figure S10 follow the expected behavior showing that the quadrupolar nature of **5** is retained in both neutral and protonated forms without the appearance of a symmetry breaking. Overall, protonation obviously favors the TPA properties leading to a more than ten times increase of δ_{TPA} for the most efficient molecule. The enhanced ICT upon protonation is the reason for this increase.

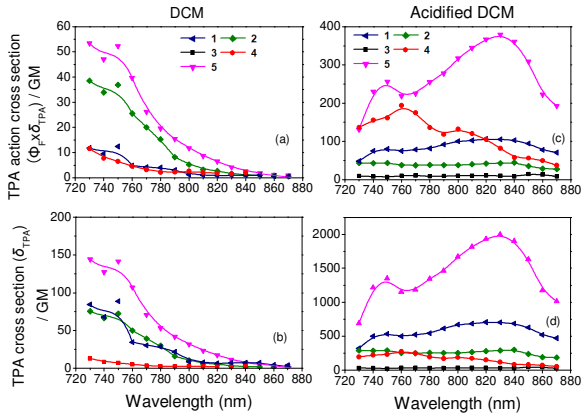

Figure 6. TPA action cross sections (a), (c) and TPA cross sections (b) and (d) of compounds **1**-**5** in DCM (a), (b) and in acidified DCM (c), (d).

Conclusions

In conclusion, five push-pull pyrimidine chromophores were studied in DCM and acidified DCM solutions, after addition of adequate amounts of TFA, focusing on their steady state, time-resolved and TPA properties. The steady state spectra showed a decrease of the absorption and fluorescence peaks of the neutral molecules and the generation of new red-shifted peaks as a consequence of the formation of protonated species. The study of the excited state dynamics, from the fs to the ns timescale, revealed a quenching of the excited states due to the enhancement of the ICT mechanism from the methoxy donors to the protonated pyrimidine acceptors. Most interestingly, the TPA properties of the compounds showed a remarkable enhancement upon protonation, reaching a ten-times increase of the δ_{TPA} of the most efficient TPA chromophore reaching 2000 GM. We believe this is an important manifestation of acid-controlled TPA properties of protonable chromophores providing a means for sensitive and non-destructive acidity sensing.

Acknowledgments

SA is grateful to the EUR LUMOMAT project and the Investments for the Future program ANR-18-EURE-0012. G.N. and SA are also grateful to the ANR ASTRID project ANR-23-ASTR-0021-02

Experimental part

The absorption spectra were recorded using a Schimadzu UV-3000 absorption spectrometer while the steady-state fluorescence spectra were recorded by using a Horiba S2 Jobin Yvon Fluoromax 4 or a Spex Fluoromax-3 Jobin-Yvon Horiba spectrofluorimeter. All fluorescence and excitation spectra were corrected to take into account the response of the photomultiplier. Fluorescence quantum yields (±10%) were determined relative to those of quinine sulfate in 0.1 M H_2SO_4 (Φ_F = 0.55), 9,10-diphenylanthracene in cyclohexane (Φ_F = 0.90), and 9,10-diphenylethynylanthracene in cyclohexane (Φ_F = 1.00).[72,73].

Two methods have been used for time resolved fluorescence measurements. The fs upconversion method providing transients in the fs-ps timescale utilized a fs mode-locked Ti:Sapphire laser with 80 fs pulses tunable from 730 to 870 nm.[74,42] The second harmonic beams at 380 or 420 nm were used for the excitation of the samples. The temporal resolution of the system was 250 fs. For the ps-ns transients, the Time Correlated Single Photon Counting method was used with a pulsed diode laser at 400 nm as the excitation source (60 ps pulse duration).[42,75] The temporal resolution of this technique was 80 ps (Fluotime 200, Picoquant). The samples for steady state and time-resolved fluorescence measurements were dilute solutions with an optical density (O.D.) of ~0.1 at excitation wavelength.

The TPA properties were studied via a TPEF technique using the same mode-locked Ti:Sapphire fs laser used for the fs upconversion measurements.[42,76,77] The samples were solutions of the chromophores in DCM and acidified DCM (2×10^{-5} M). Rhodamine 6G in MeOH (2×10^{-5}M) has been used as the reference sample, having a well-known TPA spectrum. The excitation power was changed by a set of a half-wave plate and a polarizer while the two-photon induced fluorescence was collected backwards and sent to a protomultiplier connected to photon counting electronics. The square low was always validated before calculating the TPA cross sections. The measured scattered light from the solvent has been subtracted.

Keywords: Pyrimidine • Two-photon absorption • Halochromism • Fluorescence • Time resolved spectroscopy

[1] M. Pawlicki, H. A. Collins, R. G. Denning, H. L. Anderson *Angew. Chem. Int. Ed.* **2009**, *48*, 3244–3266.
[2] G. S. He, L. S. Tan, Q. Zheng, P. N. Prasad, *Chem. Rev.* **2008**, *108*, 1245–1330.
[3] C. Xu, W. W. Webb, *J. Opt. Soc. Am B.* **1996**, *13*, 481–491.
[4] F. Terenziani, C. Katan, E. Badaeva, S. Tretiak, M. Blanchard-Desce, *Adv. Mater.* **2008**, *20*, 4641-4678.
[5] M. Rumi, J. W. Perry, *Adv. Opt. Phot.* **2010**, *2*, 451–518.
[6] M. Albota, D. Beljonne, J.-L. Brédas, J. E. Ehrlich, J. Y. Fu, A. A. Heikal, S. E. Hess, T. Kogej, M. D. Levin, S. R. Marder, D. McCord-Maughon, J. W. Perry, H. Röckel, M. Rumi, C. Subramaniam, W. W. Webb, X. L. Wu, C. Xu, *Science*, **1998**, *281*, 1653–1656.
[7] F. Terenziani, A. Painelli, C. Katan, M. Charlot, M. Blanchard-Desce, *J. Am. Chem. Soc.* **2006**, *128*, 15742–15755.
[8] L. Xu, J. Zhang, L. Yin, X. Long, W. Zhang, Q. Zhang J. *Mater. Chem. C*, 2020, 8, 6342-6349.
[9] S. Pascal, S. David, C. Andraud, O. Maury, *Chem. Soc. Rev.* **2021**, *50*, 6613–6658.
[10] Q. Liu, B. Guo, Z. Rao, B. Zhang, J. R. Gong, *Nano Lett.* **2013**, *13*, 2436–2441.
[11] A. Picot, A. D'Aleo, P. L. Baldeck, A. Grichine, A. Duperray, C. Andraud, O. Maury, *J. Am. Chem. Soc.* **2008**, *130*, 1532–1533.
[12] J. Shaya, P. R. Corridon, B. Al-Omari, A. Aoudi, A. Shunnar, M. I. H. Mohideen, A. Qurashi, B. Y. Michel, A. Burger, *J. Photochem. Photobiol. C* **2022**, *52*, 100529.
[13] A. K. Singh, A. V. Nair, N. D. Pradeep Singh, *Anal. Chem.* **2021**, *94*, 177–192.
[14] Y. Shen, A. J. Shuhendler, D. J. Ye, J. J. Xu, H. Y. Chen, *Chem. Soc. Rev.* **2016**, *45*, 6725–6741.
[15] H. A. Collin, M. Khurana, E. H. Moriyama, A. Mariampillai, E. Dahlstedt, M. Balaz, M. K. Kuimova, M. Drobizhev, V. X. D. Yang, D. Phillips, A. Rebane, B. C. Wilson, H. L. Anderson, *Nat. Photonics* **2008**, *2*, 420–424.
[16] V. Juvekar, C. S. Lim, D. J. Lee, S. J. Park, G. O. Song, H. Kang, H. M. Kim, *Chem. Sci.* **2021**, *12*, 427–434.
[17] J. E. Ehrlich, X. L. Wu, I. Y. S. Z. Y. Hu, H. Röckel, S. R. Marder, J. W. Perry, *Opt. Lett.* **1997**, *22*, 1843–1845.
[18] W. Feng, K. Liu, J. Zang, G. Wang, R. Miao, L. Ding, T. Liu, J. Kong, Y. Fang, *ACS Appl. Mater. Interfaces* **2021**, *13*, 28985–28995.
[19] J. Zheng, Z. Cao, M. Lei, Z. Nie, Y. Yang, X. Liu, B. Xu, *J. Mater. Chem. C* **2023**, *11*, 3342–3353.
[20] S. Maruo, O. Nakamura, S. Kawata, *Opt. Lett.* **1997**, 22, 132–134.
[21] B. H. Cumpston S. P. Ananthevel, S. Barlow, D. L. Dyer, J. E. Ehrlich, L. L. Erskine, A. A. Heikal, S. M. Kuebler, I. Y. S. Lee, D. McCord-Maughon, J. Q. Qin, H. Röckel, M. Rumi, X. L. Wu, S. R. Marder, J. W. Perry, *Nature* **1999**, *398*, 51–54.
[22] V. Harinarayana, Y.C. Shin *Opt. Laser Techn.* **2021**, *142*, 107180.
[23] A. Nakayama, Y. Kumamoto, M. Minoshima, K. Kikuchi, A. Taguchi, K. Fujita, *Adv. Opt. Mater.* **2022**, *10*, 2200474.
[24] A. S. Dvornikov, E. P. Walter, P. M. Rentzepis, *J. Phys. Chem. A.* **2009**, *113*, 13633–13644.
[25] Q. Geng, D. Wang, P. Chen, S.-C. Chen *Nature Commun.* **2019**, *10*, 2179.

[26] Y. Zhang, Y. Su, Y. Zhao, Z. Wang, C. Wang *Small* **2022**, *18*, 2200514.
[27] F. A. Rerza-González, E. Villatoro, M. M. Reza, J. Jara-Cortés, H. García-Ortega, E. F. Blanco-Acuña, J. G. López-Cortés, N. Esturau-Escofet, A. Aguirre-Soto, J. Peon, *Chem. Sci.* **2023**, *14*, 5783–5794.
[28] H. Sotome, T. Nagasaka, T. Konishi, K. Kamada, M. Morimoto, M. Irie, H. Miyasaka, *Photochem. Photobiol Sci.***2024**, *23,* 1041–1050.
[29] K. Mutoh, Y. Kobayashi, T. Yamane, T. Ikezawa, J. Abe, *J. Am. Chem. Soc.* **2017**, *139*, 4452–4461.
[30] E. H. Ghazvini Zadeh, S. Tang, A. W. Wondward, T. Liu, M. V. Bondar, K. D. Belfield *J. Mater. Chem. C* **2015**, *3*, 8495–8503.
[31] S. Achelle, J. Rodríguez-López, F. Robin-le Guen *Org. Biomol. Chem.* **2023**, *21*, 39–52.
[32] S. Achelle, M. Hodée, J. Massue, A. Fihey, C. Katan, *Dyes Pigm.* **2022**, *200*, 110157.
[33] L. Yu, C. Yang, *J. Mater. Chem. C* **2021**, *9*, 17265–17286.
[34] R. Komatsu, H. Sasabe, J. Kido, *J. Photonics Ener.* **2018**, *8*, 032108.
[35] E. V. Verbitskiy, G. L. Rusinov, O. N. Chupakhin, V. N. Charushin, *Dyes Pigm.* **2020**, *180*, 108414.
[36] M. Fecková, P. le Poul, F. Robin-le Guen, S. Achelle, *Dyes Pigm.* **2020**, *182*, 108659.
[37] M. Klikar, D. Georgiou, I. Polyzos, M. Fakis, Z. Růžičková, O. Pytela, F. Bureš *Dyes Pigm.* **2022**, *201*, 110230.
[38] P. Savel, H. Akdas-Kilig, J.-P. Malval, A. Spangenberg, T. Roisnel, J.-L. Fillaut, *J. Mater. Chem. C* **2014**, *2*, 295–305.
[39] B. Liu, H.-L. Zhang, J. Liu, Y.-D. Zhao, Q.-M. Luo, Z.-L. Huang, *J. Mater. Chem.* **2007**, *17*, 2921–2929.
[40] PH. H. Doan, D. R. G. Pitter, A. Kocher, J. N. Wilson, T. Goodson III, *J. Am. Chem. Soc.* **2015**, *137*, 9198–9201.
[41] L. Li, J. Ge, H. Wu, Q.-H. Xu, S. Q. Yao, *J. Am. Chem. Soc.* **2012**, *134*, 12517–12167.
[42] C. Tang, Q. Zhang, D. Li, J. Zhang, P. Shi, S. Li, J. Wu, Y. Tian, *Dyes Pigm.* **2013**, *99*, 20–28.
[43] F. Kournoutas, A. Fihey, J.-P. Malval, A. Spangenberg, M. Fecková, P. le Poul, C. Katan, F. Robin-le Guen, F. Bureš, S. Achelle, M. Fakis, *Phys. Chem. Chem. Phys.* **2020**, *22*, 4165–4176.
[44] H. Wang, Q. Zhang, J. Zhang, L. Li, Q. Zhang, S. Li, S. Zhang, J. Wu, Y. Tian, *Dyes Pigm.* **2014**, *102*, 263–272.
[45] S. Achelle, J. Rodríguez-López, F. Bureš, F. Robin-le Guen *Chem. Rec.* **2020**, *20*, 440–451.
[46] S. Achelle, J. Rodríguez-López, C. Katan, F. Robin-le Guen *J. Phys. Chem. C* **2016**, *120*, 26986–26995.
[47] M. Hodée, A. Lenne, J. Rodríguez-López, F. Robin-le Guen, C. Katan, S. Achelle, A. Fihey, *New J. Chem.* **2021**, *45*, 19132–19144.
[48] S. Achelle, J. Rodríguez-López, N. Cabon, F. Robin-le Guen, *RSC Adv.* **2015**, *5*, 107396–107399.
[49] S. Achelle, I. Nouira, B. Pfaffinger, Y. Ramondenc, N. Plé, J. Rodríguez-López, *J. Org. Chem.* **2009**, *74*, 3711–3717.
[50] S. Achelle, A. Barsella, C. Baudequin, B. Caro, F. Robin-le Guen, *J. Org. Chem.* **2012**, *77*, 4087–4096.
[51] S. Achelle, A. Barsella, B. Caro, F. Robin-le Guen, *RSC Adv.* **2015**, *5*, 39218–39227.
[52] F. Kournoutas, I. K. Kalis, M. Fecková, S. Achelle, M. Fakis, *J. Photochem. Photobiol. A* **2020**, *391*, 112398.
[53] D. Liu, Z. Zhang, H. Zhang, Y. Wang *Chem. Commun.* **2013**, *49*, 10001-10003
[54] T. P. Gerasimova, A. R. Sirazieva, S. A. Katsyuba, A. A. Kalinin, L. N. Islamova, G. M. Fazleeva, A. A. Shustikov, A. G. Shmelev, A. B. Dobrynin, O. G. Sinyashin, *Dyes Pigm.* **2023**, *210*, 110949.
[55] S. Gupta, M. D. Milton, *Dyes Pigm.* **2021**, *195*, 109690.
[56] J. T. Buck, R. W. Wilson, T. Mani, *J. Phys. Chem. Lett.* **2019**, *10*, 3080–3086.
[57] T. Ryu, K. Miyata, M. Saigo, Y. Shimoda, Y. Tsuchiya, H. Nakanotani, C. Adachi, K. Onda *Chem. Phys. Lett.* **2022**, *809*, 140155.
[58] P. K. Singh, S. Nath, M. Kumbhakar , A. C. Bhasikuttan, H. Pal, *J. Phys. Chem. A* **2008**, *112*, 5598 -5603.
[59] V. Maffeis, R. Brisse, V. Labet, B. Jousselme, T. Gustavsson *J. Phys. Chem. A* **2018**, *122*, 5533–5544.
[60] A. Cesaretti, T. Bianconi, M. Coccimiglio, N. Montegiove, Y. Rout, P. Gentili, R. Misra, B. Carlotti, *J. Phys. Chem. C* **2022**, *126*, 10429–10440.
[61] M. Bixon, J. Jortner, J. Cortes, H. Heitele M. E. Michel-Beyerle *J. Phys. Chem.* **1994**, *98*, 7289–7299.
[62] C. Ma, Y.-Q. Ou, C. T.-L. Chan, A. K.-W. Wong, R. C.-T. Chan, B. P.-Y. Chung, C. Jiang, M.-L. Wang, W.-M. Kwok, *Phys. Chem. Chem. Phys.* **2018**, *20*, 1240–1251.
[63] W. Hu, X. Miao, H. Tao, A. Baev, C. Ren, Q. Fan, T. He, W. Huang, P. N. Prasad, *ACS Nano* **2019**, *13*, 12006–12014.
[64] N. Richy, S. Gam, S. Messaoudi, A. Triadon, O. Mongin, M. Blanchard-Desce, C. Latouche, M. G. Humphrey, A. Boucekkine, J.-F. Halet, F. Paul, *Photochem* **2023**, *3*, 127–154.
[65] M. Rosendale, J. Daniel, F. Castet, P. Pagano, J.-B. Verlhac, M. Blanchard-Desce, *Molecules* **2022**, *27*, 2230.
[66] C. Tran, N. Berqouch, H. Dhimane, G. Clermont, M. Blanchard-Desce, D. Ogden, P. I. Dalko, *Chem. Eur. J.* **2017**, *23*, 1860–1868.
[67] A. I. Ciuciu, D. Firmansyah, V. Hugues, M. Blanchard-Desce, D. T. Gryko, L. Flamigni *J. Mater. Chem. C* **2014**, *2*, 4552–4565.
[68] P. Kowalczyk, M. Tasior, S. Ozaki, K. Kamada, D. T. Gryko, O*rg. Lett.* **2022**, *24*, 2551–2555.
[69] A. Cesaretti, A. Spalletti, F. Elisei, P. Foggi, R. Germani, C. G. Fortuna, B. Carlotti *Phys. Chem. Chem. Phys.* **2021**, *23*, 16739–16753
[70] Y. Rout, A. Cesaretti, E. Ferraguzzi, B. Carlotti, R. Misra *J. Phys. Chem. C* **2020**, *124*, 24631–24643.
[71] C. Katan, F. Terenziani, O. Morgin, M. H. V. Werts, L. Porrès, T. Pons, J. Mertz, S. Tretiak, M. Blanchard-Desce *J. Phys. Chem. A* **2005**, *109*, 3024–3037.
[72] M. Taniguchi, J. S. Lindsey, *Photochem. Photobiol.* **2018**, *94*, 290–327.

[73] D. F. Eaton, *Pure Appl. Chem.* **1988**, *60*, 1007–1114.
[74] V. Petropoulos, I. Georgoulis, C. Vourdaki, P. Hrobárik, I. Sigmundová, J. Nociarová, M. Maiuri, G. Cerullo, M. Fakis. *ChemPhysChem* **2023**, *24*, e202300127
[75] M. Fecková, I. K. Kalis, T. Roisnel, P. le Poul, O. Pytela, M. Klikar, F. Robin-le Guen, F. Bureš, M. Fakis, S Achelle, *Chem. Eur. J.* **2021**, *13*, 1145–1159.
[76] N. S. Makarov, M. Drobizhev, A. Rebane, *Opt. Express* **2008**, *16*, 4029–4047.
[77] J. Nociarova, P. Osusky, E. Rakovsky, D. Georgiou, I. Polyzos, M. Fakis, P. Hrobarik, *Org. Lett.* **2021**, *23*, 3460–3465.

Entry for the table of contents

Protonation of a styrylpyrimidine quadrupolar chromophore increases the two-photon absorption cross section more than ten times reaching 2000 GM.